frontiers | Frontiers in Molecular Biosciences

TYPE Brief Research Report
PUBLISHED 06 January 2023
DOI 10.3389/fmolb.2022.1098144

OPEN ACCESS

EDITED BY
Simin Rahighi,
Chapman University, United States

REVIEWED BY
David Reverter,
Universitat Autònoma de Barcelona, Spain
Wei Zhang,
University of Guelph, Canada

*CORRESPONDENCE
Katrin Rittinger,
katrin.rittinger@crick.ac.uk
Benjamin Stieglitz,
benjamin.stieglitz@qmul.ac.uk

†PRESENT ADDRESS
Qilong Wu,
Centre for Medicines Discovery, University of Oxford, Oxford, United Kingdom
Marios G. Koliopoulos,
Division of Structural Biology, Chester Beatty Laboratories, The Institute of Cancer Research, London, United Kingdom

SPECIALTY SECTION
This article was submitted to Protein Biochemistry for Basic and Applied Sciences, a section of the journal Frontiers in Molecular Biosciences

RECEIVED 14 November 2022
ACCEPTED 19 December 2022
PUBLISHED 06 January 2023

CITATION
Wu Q, Koliopoulos MG, Rittinger K and Stieglitz B (2023), Structural basis for ubiquitylation by HOIL-1.
Front. Mol. Biosci. 9:1098144.
doi: 10.3389/fmolb.2022.1098144

Structural basis for ubiquitylation by HOIL-1

Qilong Wu[1†], Marios G. Koliopoulos[2†], Katrin Rittinger[2*] and Benjamin Stieglitz[1*]

[1]Department of Biochemistry, School of Biological and Behavioural Sciences, Queen Mary University of London, London, United Kingdom, [2]Molecular Structure of Cell Signalling Laboratory, The Francis Crick Institute, London, United Kingdom

The linear ubiquitin chain assembly complex synthesises linear Ub chains which constitute a binding and activation platform for components of the TNF signalling pathway. One of the components of LUBAC is the ubiquitin ligase HOIL-1 which has been shown to generate oxyester linkages on several proteins and on linear polysaccharides. We show that HOIL-1 activity requires linear tetra-Ub binding which enables HOIL-1 to mono-ubiquitylate linear Ub chains and polysaccharides. Furthermore, we describe the crystal structure of a C-terminal tandem domain construct of HOIL-1 comprising the IBR and RING2 domains. Interestingly, the structure reveals a unique bi-nuclear Zn-cluster which substitutes the second zinc finger of the canonical RING2 fold. We identify the C-terminal histidine of this bi-nuclear Zn-cluster as the catalytic base required for the ubiquitylation activity of HOIL-1. Our study suggests that the unique zinc-coordinating architecture of RING2 provides a binding platform for ubiquitylation targets.

KEYWORDS

ubiquitin, LUBAC, HOIL-1L, HOIP, RBCK1, E3 ligase, TNF signalling, amylopectinosis

Introduction

Stimulation of innate and adaptive immune receptors trigger the activation of multiple ubiquitin ligases which orchestrate the initiation of inflammatory gene expression by transcription factor NF-κB (Haas et al., 2009). Among those E3 enzymes with essential roles in NF-κB activation is the linear ubiquitin chain assembly complex, LUBAC, which attaches linear (or M1-linked) ubiquitin chains to a set of target proteins (Hrdinka and Gyrd-Hansen, 2017). In contrast to canonical ubiquitin chains which are linked by isopetide bonds between lysine residues and the C-terminal glycine of ubiquitin, M1-Ub chains are generated in a head-to-tail fashion by creating a peptide bond between the N-terminal methionine and C-terminus of the two adjoining Ub moieties. LUBAC is a heterotrimeric ligase which consists of the three proteins HOIP, HOIL-1 (also known as RBCK1) and SHARPIN (Gerlach et al., 2011; Ikeda et al., 2011; Tokunaga et al., 2011). Two of the LUBAC components display Ub ligase activity, HOIP and HOIL-1, and both belong to the family of RBR (Ring-between-RING) ligases. Their catalytic activity resides within a specific combination of three domains: a canonical RING1 domain is followed by two zinc coordinating domains termed IBR (In-between-RING) and RING2. The structural and mechanistic features of this RBR catalytic module have been extensively investigated (Walden and Rittinger, 2018; Cotton and Lechtenberg, 2020). RBR ligases recruit Ub charged E2 enzymes *via* the RING1 domain. The activated ubiquitin is then moved in a transthiolation reaction from the E2 onto a conserved cysteine located in the first zinc-coordinating loop of the RING2 domain to form a thioester intermediate between ubiquitin and the RBR ligase. Substrate binding near the Ub-thioester intermediate allows an aminolysis reaction to occur which attaches Ub to the target

protein. Linear Ub chain synthesis by LUBAC is carried out by the ligase component HOIP which binds to an acceptor Ub molecule in the vicinity of the Ub-thioester at the RING2 domain that leads to formation of a peptide bond between the C-terminus of the donor Ub and the N-terminus of the acceptor Ub (Smit et al., 2012; Stieglitz et al., 2012). The reaction proceeds *via* a nucleophilic attack from the N-terminal methionine of the acceptor Ub which is assisted by a catalytic base in form of a histidine located near the catalytic cysteine, a mechanism which is widely conserved among RBR ligases (Stieglitz et al., 2013). Interestingly, several studies of the LUBAC component HOIL-1 have now demonstrated that its activity deviates from canonical RBR ligases by eliciting a unique functionally. It has been shown that HOIL-1L mono-ubiquitylates several immune signaling proteins such as MyD88 (Myeloid differentiation factor 88), the IL-1 receptor associated kinases IRAK1and IRAK2 by catalyzing formation of an ester bond between the hydroxy group of serine or threonine residues and the C-terminal glycine of Ub. Moreover, ester-linked ubiquitylation was also reported to take place on ubiquitin itself at T12, S20, T22 and T55, which may have important consequences for the catalytic activity of LUBAC (Kelsall et al., 2019; Carvajal et al., 2021). HOIL-1 mediated ester-linked ubiquitylation of the distal Ub of a linear chain cannot be further extended by HOIP due to a steric hindrance created by the ester bound Ub molecule. The discovery of HOIL-1 mediated mono-ubiquitylation by oxyester linkages on several targets proteins and on ubiquitin chains provides a new layer of complexity for the regulation of immune pathways by the ubiquitin system (Kelsall, 2022). The ester-linked ubiquitylation activity of HOIL-1 does not only play intricate roles in context of LUBAC mediated signaling but is also involved in the seemingly unrelated background of defective glycogen homeostasis. It was recently shown that HOIL-1 can ubiquitylate polysaccharides under *in vitro* conditions by attaching Ub to the hydroxy group of unbranched carbohydrates (Kelsall et al., 2022). This intriguing feature provides a rationale for several clinical case studies that have uncovered a genetic link between HOIL-1 deficiencies and glycogen storage diseases (Boisson et al., 2012; Krenn et al., 2018; Phadke et al., 2020; Nitschke et al., 2022). Although the discovery of the unique ubiquitylation activity of HOIL-1 represents a major advancement in our knowledge about the diverse functionality of RBR ligases, its structural and mechanistic basis has not been explored. To understand the molecular requirements which enable HOIL-1 to catalyze the attachment of Ub to proteins or carbohydrates by oxyester linkages, we have solved the crystal structure of a C-terminal tandem domain construct comprising the IBR and RING2 domain and identify a unique Zn-cluster as molecular feature required for catalysis.

Materials and methods

Protein expression, labelling and purification

All constructs were expressed and purified as described previously (Stieglitz et al., 2012). Point mutations were generated using the QuikChange site-directed mutagenesis kit (Stratagene). All plasmids were verified by DNA sequencing. Protein concentrations were determined by UV-VIS Spectrophotometry at 280 nm using calculated extinction coefficients. Bovine mono-ubiquitin was purchased from Sigma and further purified by SEC. Ubiquitin R54C was labelled at position R54 by introducing a cysteine by site-directed mutagenesis. Labeling was carried out with Cy5 maleimide mono-reactive dye (Cytiva) according to the manufacturer's instructions with subsequent purification by SEC.

Ubiquitylation assays

Assays were performed using 1 μM E1, 10 μM UbcH, 7.5 μM HOIP 694-1072 and/or 5 μM HOIL-1, 30 μM Ub, 1 μM Ub R54C-Cy5 and 10 mM maltoheptaose. Reactions were incubated at 25°C in 50 mM HEPES pH 7.4 with 150 mM NaCl. Samples were taken at 5, 10, 15, 30, and 60 min after addition of 5 mM ATP. Reactions were quenched by snap-freezing in liquid nitrogen and analyzed by SDS-PAGE using an iBright Imaging System (Thermo Fisher Scientific) for visualization of Coomassie Brilliant blue, Lumitein or Cy5.

Isothermal titration calorimetry

ITC measurements were performed using PEAQ-ITC micro calorimeter (Malvern Panalytical). All samples were dialyzed into buffer containing 50 mM HEPES pH 7.5, 150 mM NaCl and 1 mM TCEP. Titrations were performed at 20°C with 50 μM of HOIL-1 loaded into the cell and 500 μM linear tetra Ub into the syringe.

Crystallization, data collection and structure determination

Crystallization trials with HOIL-1 residues 366–510 were set up at 10 mg/mL using an Oryx crystallization robot. Initial hits were optimized by sitting-drop vapor diffusion at 18°C with a reservoir solution containing 200 mM magnesium chloride hexahydrate, 100 mM Tris-HCl pH 7.0, 10% (w/v) PEG 8000. Crystals were flash-frozen in the reservoir solution containing 30% glycerol. Crystals of HOIL-1 (366–510) diffracted to 2.44 Å. A data set was collected on beamline IO2 at the Diamond Light Source (Oxford, United Kingdom) and processed using XDS (Kabsch, 2010). The structure was solved by Zn^{2+}-SAD phasing. Heavy-atom search, density modification and initial model building was performed using Phenix AutoSol (Adams et al., 2010). The model was iteratively improved by manual building in Coot and refined using REFMAC5 and Phenix (Murshudov et al., 1997; Emsley and Cowtan, 2004). The stereochemistry of the final models was analyzed with Procheck (Laskowski et al., 1993). Data collection and refinement statistics are collated in Supplementary Table S1. Structural figures were prepared in PyMOL (Schrödinger and DeLano, 2020). The atomic coordinates and structure factors for the crystal structure of HOIL-1 (366–510) have been deposited with the Protein Data bank under the accession number 8BVL.

Results

In vitro reconstitution of HOIL-1 ubiquitylation activity

We have previously shown that HOIP is the principal LUBAC component which catalyzes the formation of linear Ub chains (Stieglitz et al., 2013). In contrast, HOIL-1 displays only poor ligase

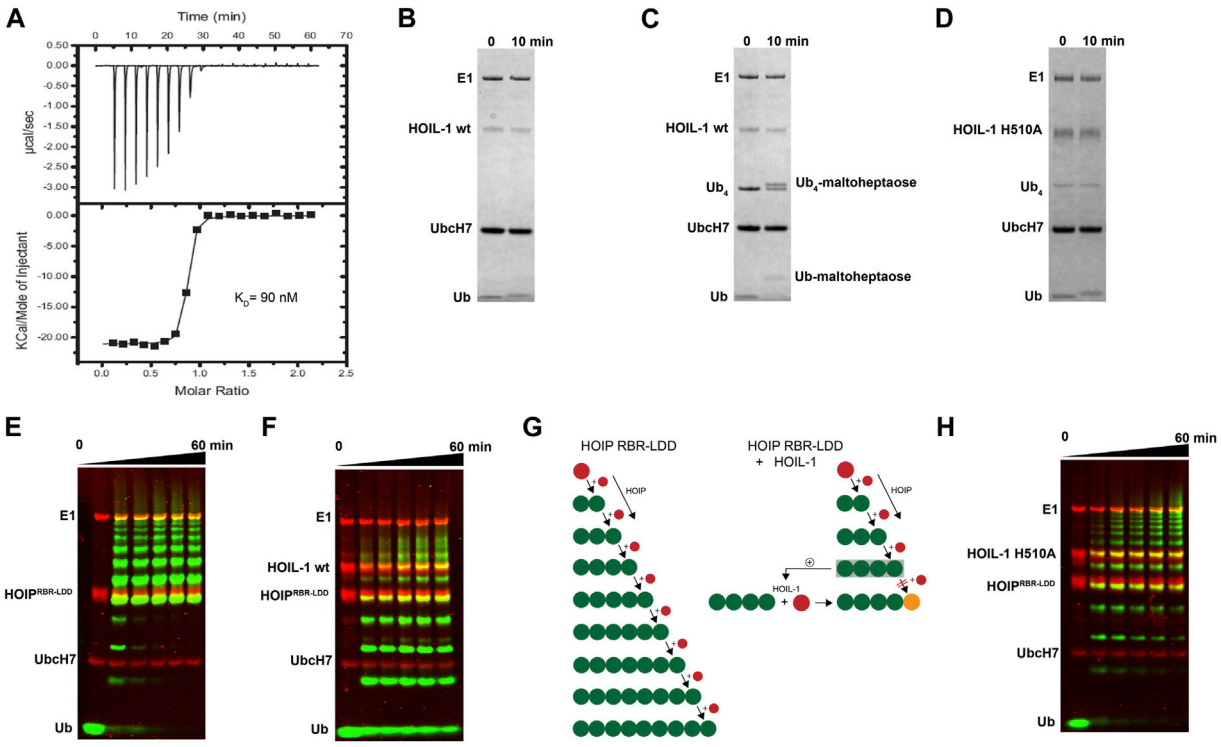

FIGURE 1
In vitro reconstitution of HOIL-1 ubiquitylation activity. **(A)** Quantitative measurement of HOIL-1 binding to linear Ub_4 by ITC (K_D = 90 nM). Carbohydrate ubiquitylation of HOIL-1 in the absence **(B)** and presence **(C)** of linear tetra Ub. **(D)** The mutation H510A abolishes carbohydrate ubiquitylation of HOIL-1. **(E)** *In vitro* reconstitution of HOIP-RBR-LDD (residues 697–1072) ligase activity. **(F)** The linear ubiquitin chain synthesis activity of HOIP-RBR-LDD is restricted in the presence of HOIL-1 wt. **(G)** The ubiquitylation activities of HOIP-LDD and HOIL-1 are schematically illustrated with mono-Ub in red, linear Ub in green and ester linked Ub in orange. HOIL-1 is stimulated by linear tetra Ub as indicated by a plus symbol. **(H)** HOIP-LDD mediated linear Ub chain synthesis is re-established in the presence of HOIL-1 H510A.

activity and is dispensable for linear Ub chains synthesis (Smit et al., 2012; Stieglitz et al., 2012). However, several studies have recently reported that HOIL-1 exhibits a robust ester-linked ubiquitylation activity for linear Ub chains as well as maltoheptaose, which acts as a proxy for unbranched polysaccharides (Kelsall, 2022). Both types of ubiquitylation activities depend on the presence of linear tetra-Ub which binds to HOIL-1 with nanomolar affinity (Figure 1A) and might act as an allosteric activator (Kelsall et al., 2022). The modification of maltoheptaose can be readily detected in an *in vitro* reconstitution system which consists of purified components of the ubiquitylation cascade. Ubiquitylation of maltoheptaose is observed after 10 min in the presence of tetra-Ub (Figure 1B, C). To observe ester-linked ubiquitylation of ubiquitin, we have set up an assay which takes advantage of the inhibitory effect of oxyester branched Ub chains on HOIP activity. The isolated RBR module of HOIP displays ubiquitylation activity until the entire pool of mono Ub has been converted into linear poly-Ub chains with molecular weights corresponding to chain lengths of 5–12 Ub molecules (Figure 1E). In contrast, the linear chains which are synthesized in the presence of HOIL-1 are much shorter which predominantly consist of chains of 2–6 Ub moieties (Figure 1F). Even after 60 min the mono Ub pool is not depleted, indicating the presence of HOIL-1 restricts the linear Ub chain synthesis activity of HOIP. This result is in agreement with a recent study which demonstrates that HOIL-1 ubiquitylates tetra-Ub on Thr12 and Thr55 which creates a steric block for further chain elongation by HOIP (Carvajal et al., 2021). Thus, the reconstitution of linear chain synthesis in the presence of HOIP-RBR and HOIL-1 allows two competing reactions to occur (Figure 1G): First, HOIP generates linear Ub chains from mono Ub. Once tetra-Ub is formed it can act as an allosteric activator for HOIL-1 which adds a molecule of Ub to linear Ub chains *via* an oxy-ester linkage, thereby blocking HOIP from further linear chain elongation. Our analysis of HOIL-1 ligase activity is in line with recent studies which demonstrate a distinct functionality for HOIL-1, which deviates from other RBR ligases who catalyze amide-linked ubiquitylation.

Structural characterization of the HOIL-1 IBR-RING2 tandem domain

To understand the molecular determinants for HOIL-1 specific ubiquitylation we analyzed the sequence of HOIL-1 with a focus on the region in immediate vicinity to the catalytic cysteine (Cys460) of the RING2 domain (Figure 2A). A sequence alignment revealed that HOIL-1 together with HOIP, RNF216, and RNF144 deviates in the otherwise conserved pattern of Zn-coordinating residues downstream of the catalytic cysteine. For HOIP and RNF216 this is not surprising since their structures display zinc finger insertions in RING2 which have been shown to be essential for their catalytic activity of M1-linked and K69-linked Ub chain synthesis (Stieglitz et al., 2013; Cotton et al., 2022). This suggests that HOIL-1 also

10.3389/fmolb.2022.1098144

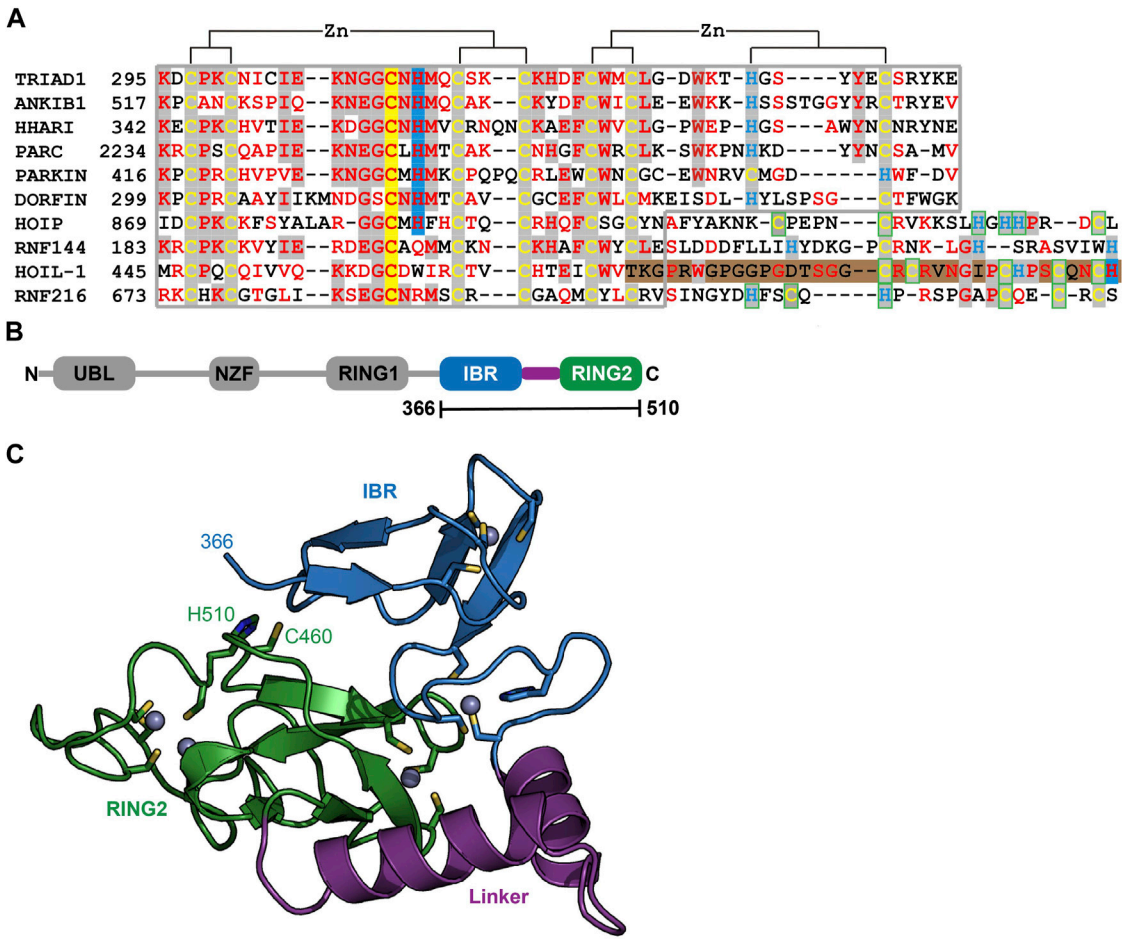

FIGURE 2
Structural characterization of HOIL-1 shows a unique deviation of the RING2 domain. **(A)** The RING2 domains of human RBR domains have been aligned according to conserved Zn^{2+} coordinating residues. Catalytic cysteine and histidine residues are depicted on a yellow and blue background, respectively. The C-terminal binuclear Zn-cluster of HOIL-1 is represented on a brown background. **(B)** Domain architecture of HOIL-1 illustrates the boundaries of the crystallized construct. (Domain acronyms: UBL, ubiquitin like domain; NZF, Npl4 zinc finger; RING1/2, really interesting new gene domain; IBR = in between RING domain). **(C)** Structural model of residues 366–510 of HOIL-1 as ribbon models with Zn^{2+} ions as grey spheres. Zn^{2+} coordinating residues, the catalytic cysteine and histidine are shown as a stick model.

features a unique Zn-chelating structure within the C-terminal part of RING2 which is potentially important for HOIL-1 catalytic activity. This notion is further supported by a clinical study which reports two patients with amylopectinosis who carry mutations at position 498 or 508 in RING2 of HOIL-1L (Nitschke et al., 2022). In addition, unlike most RBR ligases, HOIL-1 does not display a histidine next to the conserved catalytic cysteine which suggests that its catalytic mechanism differs from canonical RBRs. To elucidate the structural features which enable HOIL-1 to exert its unique catalytic activity we solved the crystal structure of fragment 366–510, which comprises the IBR and the RING2 domain (Figure 2B; Supplementary Table S1). The overall structure shows that both domains are linked by two helices, which are positioned at a 50 angle (Figure 2C). This arrangement brings the IBR and the RING2 domains into close vicinity to each other and allows them to form an interface which buries a total of 1,303 A^2 of solvent accessible surface area. The interface is formed by hydrophobic and electrostatic interactions between the N-terminal part of RING2 and the loop regions adjacent to the four beta-strands of the IBR domain (Figure 3A). K457 of RING2 is a central contact point for the IBR domain, and is coordinated by F382, E383, V386, and N387. The C-terminal histidine (H510) of RING2 forms a polar interaction with D385 of the IBR domain. These interactions, together with further hydrophobic and polar contributions by D458, K456, Q455, I452, V467, and R464 in RING2 with N387, K403, and L401 of the IBR, create a surface which largely obstructs the catalytic cysteine C460. We therefore assume that the observed structural arrangement represents a catalytic inactive conformation of HOIL-1 in which the catalytic cysteine of RING2 is masked by the IBR domain. As expected from our sequence analysis, the C-terminal part of the RING2 domain of HOIL-1L reveals a unique architecture not observed in other RBR ligases so far: The C-terminal 36 residues form a loop structure which is laced up by a binuclear Zn cluster coordinated by six cysteines (Figure 3B). This structure adopts a compact conformation which packs against the second beta sheet of the canonical RING2 fold. HOIL-1 displays a tryptophan (W462) instead of a histidine located two amino acids downstream of the catalytic cysteine (Figure 2A), questioning if HOIL-1 requires a

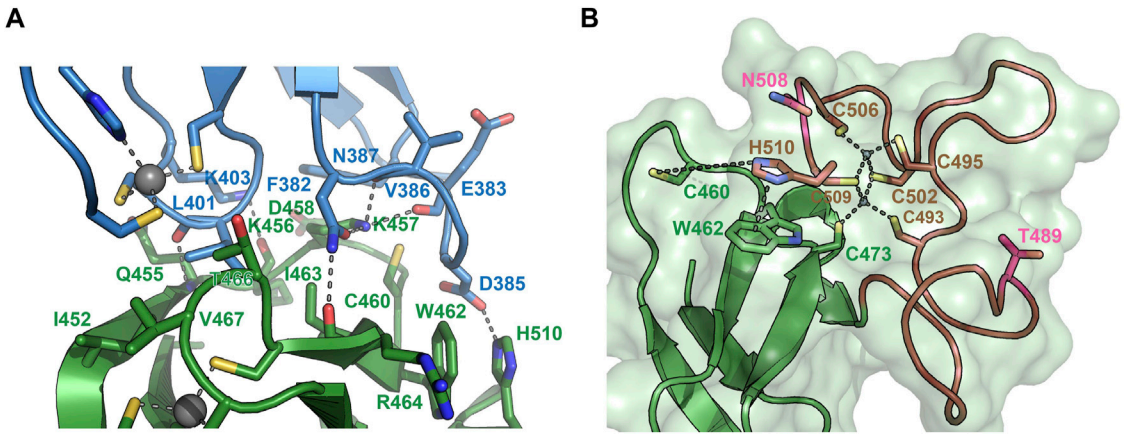

FIGURE 3
Structural details of the HOIL-1 IBR-RING2 architecture. **(A)** Close-up view of the interface between the IBR domain (blue) and the RING2 domain (green). Residues involved in IBR-RING2 interactions are shown as sticks. The catalytic cysteine (C460) protrudes into a groove of the IBR surface. Polar interactions are shown as dashed lines. The cut-off distance for polar and hydrophobic interactions is 3.5 and 4 Å, respectively. **(B)** Close-up view of the C-terminal loop region of RING2 which form the binuclear Zinc-cluster (brown). Zinc coordinating interactions with cysteines are shown as dashed lines. The pi-stacking interaction between H501and W462 is shown as dashed line. The distance between H510 and the catalytic cysteine 460 is 7.6 Å. Positions for pathogenic variants of HOIL-1 (Thr489Profs*9 and Asn508Profs*4) in patients with polyglucosan storage disorders 489 and 508 are shown in pink.

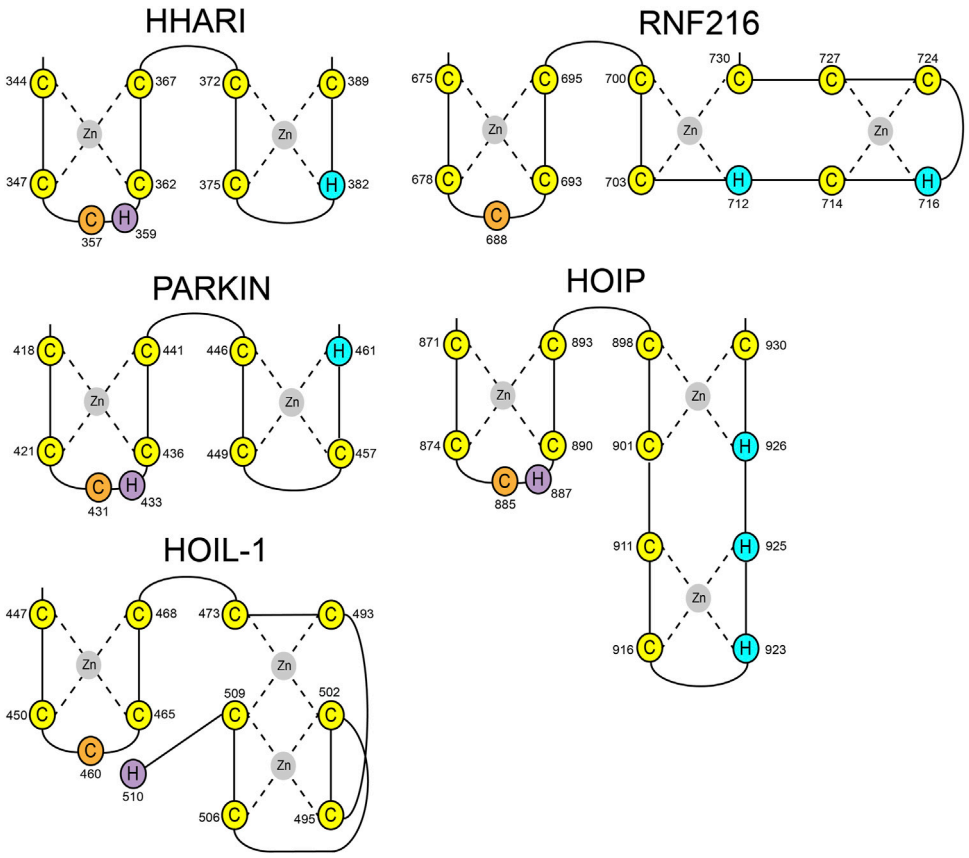

FIGURE 4
Schematic presentation of RING2 topologies of the RBR ligases HHARI, Parkin, HOIP, RNF216, and HOIL-1. Zinc coordinating cysteine and histidine residues are shown in yellow and blue, respectively. Catalytic cysteines are shown in orange. Catalytic histidine residues have been identified for HHARI, Parkin, HOIP, and HOIL-1 (magenta).

histidine to assist catalysis as observed for other RBR ligases. The loop region of RING2, which wraps around the bi-nuclear Zn-cluster, terminates next to W462. The C-terminal residue of HOIL-1 is a histidine (H510) which forms a pi-staking interaction with W462. In this configuration H510 is ideally positioned to act as a catalytic base. To probe the relevance of H510 for HOIL-1 catalysis, we tested the mutant H510A in our *in vitro* reconstitution assay. Strikingly, this mutant is unable to ubiquitylate maltoheptaose and shows a strongly reduced ability to inhibit HOIP mediated linear Ub chain synthesis, indicating that H510 is required for HOIL-1 catalytic activity (Figures 1D, H).

Discussion

HOIL-1 is a member of the RBR E3 ligase family with the ability to ubiquitylate its targets by linking a hydroxy group of the substrate to the C-terminus of Ub. The recent discovery that the resulting ester bonds cannot only be created on proteins but also on carbohydrates, opens new possibilities for the ubiquitin system beyond its definition as a posttranslational modification. Our study sheds light on the structural requirements for the ligase activity of HOIL-1 and uncovers a notable variation of the ubiquitin transfer activity in RBR ligases. Several studies have demonstrated that RBR ligases utilize a histidine as a general base for catalysis, which is located in the first zinc coordinating loop of RING2 next to the catalytic cysteine (Figure 4) (Cotton and Lechtenberg, 2020). HOIL-1 displays a tryptophan in this position but instead provides the catalytic histidine *via* a unique structural feature not observed in any other RBR ligase. Our structural and biochemical analysis identifies the C-terminal H510 as the catalytic base in HOIL-1. The residue is placed next to the catalytic cysteine through a stretch of 37 residues which fold into a binuclear zinc-cluster. We hypothesize that the extended loop structure of the C-terminal zinc-cluster creates a substrate binding platform for HOIL-1. Specific substrate binding domains have not been identified for any RBR ligase. Based on structural studies on other RBR members such as HOIP, RNF216, and HHARI it becomes increasingly evident that the C-terminal half of RING2 next to the first zinc finger generally determines the substrate specificity in RBR ligases (Stieglitz et al., 2013; Cotton et al., 2022; Reiter et al., 2022; Stieglitz, 2022) (Figure 4). The discovery of the binuclear zinc cluster in RING2 of HOIL-1 supports this hypothesis. The importance of the C-terminal structural architecture for proper HOIL-1 catalysis is also highlighted by the recent identification of mutations in the bi-nuclear Zn cluster in patients with polyglucosan storage disorders (Figure 3B) (Nitschke et al., 2022). The overall structure of the HOIL-1 tandem domain construct shows that the IBR and the RING2 domains of HOIL-1 are connected by a helical segment. This observation is in-line with the structural models of other RBR ligases, which also display one or two helices to separate both domains from each other. However, in contrast to the structures HOIP, RNF216 and HHARI, which have been captured in their active conformation, the helical linker in HOIL-1 creates a hinge which brings the IBR and the RING2 domain in close contact to each other (Supplementary Figure S1) (Lechtenberg et al., 2016; Horn-Ghetko et al., 2021; Cotton et al., 2022). Since this intermolecular interaction partially obstructs the catalytic site of RING2, we speculate that the observed conformation represents a catalytic inactive conformation. In this context it is important to note that inhibition of ligase activity by intramolecular interaction between RING2 and a second domain is a common mechanistic concept in RBR ligases. For example, Parkin is auto-inhibited *via* interaction of the RING2 domain with its RING0 domain, while HHARI employs the C-terminal Ariadne domain to shield the catalytic cysteine in RING2 (Supplementary Figure S2) (Duda et al., 2013; Kumar et al., 2015). The structure of HOIL-1 might expand this paradigm with the notable variation that no additional domain outside the core RBR module is required to achieve an auto-inhibited conformation. Our biochemical analysis of HOIL-1 enzymatic function shows that the ligase requires the presence of linear tetra Ub for its activity. A previous study has shown that HOIL-1 binds linear and K63 linked Ub chains for allosteric activation and suggested that binding of allosteric Ub chains involve the IBR domain, similar to the allosteric Ub binding site observed in the structure of activated HOIP (Supplementary Figure S3) (Kelsall et al., 2022). It is tempting to speculate that binding of allosteric poly Ub at this position could dislodge the RING2 domain from the backside of the IBR domain in order to adopt a catalytic competent conformation.

In summary, we have uncovered that HOIL-1 adopts a unique structure in form of a binuclear zinc-cluster which is required for its catalytic function. To further dissect the mechanism of HOIL-1 catalysis it will be essential to obtain high-resolution structures of HOIL-1 in its active conformation bound to its substrates. Future studies need to provide an understanding how HOIL-1 is able to ubiquitylate carbohydrates in molecular detail.

Data availability statement

The original contributions presented in the study are included in the article/Supplementary Material, further inquiries can be directed to the corresponding authors.

Author contributions

KR and BS conceived the study and wrote the manuscript. QW, MK and BS performed and analyzed experiments. All authors contributed to the article and approved the submitted version.

Funding

This work was supported by the Francis Crick Institute which receives its core funding from Cancer Research UK (CC 2075), the UK Medical Research Council (CC 2075), and the Wellcome Trust (CC 2075).

Acknowledgments

We thank E. Christodoulou for technical assistance, L. Haire for help with crystallization P. Walker for data collection and the Diamond Light Source for synchrotron access.

Conflict of interest

The authors declare that the research was conducted in the absence of any commercial or financial relationships that could be construed as a potential conflict of interest.

Publisher's note

All claims expressed in this article are solely those of the authors and do not necessarily represent those of their affiliated organizations, or those of the publisher, the editors and the reviewers. Any product that may be evaluated in this article, or claim that may be made by its manufacturer, is not guaranteed or endorsed by the publisher.

Supplementary material

The Supplementary Material for this article can be found online at: https://www.frontiersin.org/articles/10.3389/fmolb.2022.1098144/full#supplementary-material

References

Adams, P. D., Afonine, P. V., Bunkoczi, G., Chen, V. B., Davis, I. W., Echols, N., et al. (2010). Phenix: A comprehensive python-based system for macromolecular structure solution. *Acta Crystallogr. Sect. D. Biol. Crystallogr.* 66 (2), 213–221. doi:10.1107/S0907444909052925

Boisson, B., Laplantine, E., Prando, C., Giliani, S., Israelsson, E., Xu, Z., et al. (2012). Immunodeficiency, autoinflammation and amylopectinosis in humans with inherited HOIL-1 and LUBAC deficiency. *Nat. Immunol.* 13 (12), 1178–1186. doi:10.1038/ni.2457

Carvajal, A. R., Grishkovskaya, I., Gomez Diaz, C., Vogel, A., Sonn-Segev, A., Kushwah, M. S., et al. (2021). The linear ubiquitin chain assembly complex (LUBAC) generates heterotypic ubiquitin chains. *eLife* 10, e606600. doi:10.7554/eLife.60660

Cotton, T. R., Cobbold, S. A., Bernardini, J. P., Richardson, L. W., Wang, X. S., and Lechtenberg, B. C. (2022). Structural basis of K63-ubiquitin chain formation by the Gordon-Holmes syndrome RBR E3 ubiquitin ligase RNF216. *Mol. Cell* 82 (3), 598–615.e8. e8. doi:10.1016/j.molcel.2021.12.005

Cotton, T. R., and Lechtenberg, B. C. (2020). Chain reactions: Molecular mechanisms of RBR ubiquitin ligases. *Biochem. Soc. Trans.* 48 (4), 1737–1750. doi:10.1042/BST20200237

Duda, D. M., Olszewski, J. L., Schuermann, J. P., Kurinov, I., Miller, D. J., Nourse, A., et al. (2013). Structure of HHARI, a RING-IBR-RING ubiquitin ligase: Autoinhibition of an Ariadne-family E3 and insights into ligation mechanism', *Structure. Elsevier Ltd.* 21 (6), 1030–1041. doi:10.1016/j.str.2013.04.019

Emsley, P., and Cowtan, K. (2004). Coot: Model-building tools for molecular graphics', *acta crystallographica section D: Biological crystallography. Int. Union Crystallogr.* 60 (12 I), 2126–2132. doi:10.1107/S0907444904019158

Gerlach, B., Cordier, S. M., Schmukle, A. C., Emmerich, C. H., Rieser, E., Haas, T. L., et al. (2011). Linear ubiquitination prevents inflammation and regulates immune signalling. *Nature* 471 (7340), 591–596. doi:10.1038/nature09816

Haas, T. L., Emmerich, C. H., Gerlach, B., Schmukle, A. C., Cordier, S. M., Rieser, E., et al. (2009). Recruitment of the linear ubiquitin chain assembly complex stabilizes the TNF-R1 signaling complex and is required for TNF-mediated gene induction. *Mol. Cell* 36 (5), 831–844. doi:10.1016/j.molcel.2009.10.013

Horn-Ghetko, D., Krist, D. T., Prabu, R. J., Baek, K., Mulder, M. P. C., Klügel, M., et al. (2021). Ubiquitin ligation to F-box protein targets by SCF–RBR E3–E3 super-assembly', *Nature. Springer U. S.* 590 (7847), 671–676. doi:10.1038/s41586-021-03197-9

Hrdinka, M., and Gyrd-Hansen, M. (2017). The met1-linked ubiquitin machinery: Emerging themes of (De)regulation. *Mol. Cell* 68, 265–280. doi:10.1016/j.molcel.2017.09.001

Ikeda, F., Deribe, Y. L., Skanland, S. S., Stieglitz, B., Grabbe, C., Franz-Wachtel, M., et al. (2011). SHARPIN forms a linear ubiquitin ligase complex regulating NF-?B activity and apoptosis. *Nature* 471 (7340), 637–641. doi:10.1038/nature09814

Kabsch, W. (2010). Research papers XDS research papers. *Acta Crystallogr. Sect. D. Biol. Crystallogr.* 66, 125–132. doi:10.1107/S0907444909047337

Kelsall, I. R., McCrory, E. H., Xu, Y., Scudamore, C. L., Nanda, S. K., Mancebo-Gamella, P., et al. (2022). HOIL-1 ubiquitin ligase activity targets unbranched glucosaccharides and is required to prevent polyglucosan accumulation. *EMBO J.* 41 (8), e109700–e109717. doi:10.15252/embj.2021109700

Kelsall, I. R. (2022). Non-lysine ubiquitylation: Doing things differently. *Front. Mol. Biosci.* 9, 1008175. doi:10.3389/fmolb.2022.1008175

Kelsall, I. R., Zhang, J., Knebel, A., Arthur, J. S. C., and Cohen, P. (2019). The E3 ligase HOIL-1 catalyses ester bond formation between ubiquitin and components of the Myddosome in mammalian cells. *Proc. Natl. Acad. Sci. U. S. A.* 116 (27), 13293–13298. doi:10.1073/pnas.1905873116

Krenn, M., Salzer, E., Simonitsch-Klupp, I., Rath, J., Wagner, M., Haack, T. B., et al. (2018). Mutations outside the N-terminal part of RBCK1 may cause polyglucosan body myopathy with immunological dysfunction: Expanding the genotype–phenotype spectrum. *J. Neurology* 265 (2), 394–401. doi:10.1007/s00415-017-8710-x

Kumar, A., Aguirre, J. D., Condos, T. E. C., Martinez-Torres, R. J., Chaugule, V. K., Toth, R., et al. (2015). Disruption of the autoinhibited state primes the E3 ligase parkin for activation and catalysis. *EMBO J.* 34 (20), 2506–2521. doi:10.15252/embj.201592337

Laskowski, R. A., MacArthur, M. W., Moss, D. S., and Thornton, J. M. (1993). Procheck: A program to check the stereochemical quality of protein structures', *Journal of applied crystallography. Int. Union Crystallogr.* 26 (2), 283–291. doi:10.1107/s0021889892009944

Lechtenberg, B. C., Rajput, A., Sanishvili, R., Dobaczewska, M. K., Ware, C. F., Mace, P. D., et al. (2016). Structure of a HOIP/E2~ubiquitin complex reveals RBR E3 ligase mechanism and regulation', *Nature. Nat. Publ. Group* 529 (7587), 546–550. doi:10.1038/nature16511

Murshudov, G. N., Vagin, A. A., and Dodson, E. J. (1997). Refinement of macromolecular structures by the maximum-likelihood method', *acta crystallographica section D: Biological crystallography. Int. Union Crystallogr.* 53 (3), 240–255. doi:10.1107/S0907444996012255

Nitschke, S., Sullivan, M. A., Mitra, S., Marchioni, C. R., Lee, J. P. Y., Smith, B. H., et al. (2022). Glycogen synthase downregulation rescues the amylopectinosis of murine RBCK1 deficiency. *Brain* 145 (7), 2361–2377. doi:10.1093/brain/awac017

Phadke, R., Hedberg-Oldfors, C., Scalco, R. S., Lowe, D. M., Ashworth, M., Novelli, M., et al. (2020). RBCK1-related disease: A rare multisystem disorder with polyglucosan storage, auto-inflammation, recurrent infections, skeletal, and cardiac myopathy—four additional patients and a review of the current literature. *J. Inherit. Metabolic Dis.* 43 (5), 1002–1013. doi:10.1002/jimd.12234

Reiter, K. H., Zelter, A., Janowska, M. K., Riffle, M., Shulman, N., MacLean, B. X., et al. (2022). Cullin-independent recognition of HHARI substrates by a dynamic RBR catalytic domain. *Struct. Elsevier Ltd.* 30 (9), 1269–1284.e6. e6. doi:10.1016/j.str.2022.05.017

Schrödinger, L., and DeLano, W. (2020). *PyMOL*. Available at: http://www.pymol.org/pymol.

Smit, J. J., Monteferrario, D., Noordermeer, S. M., van Dijk, W. J., van der Reijden, B. A., and Sixma, T. K. (2012). The E3 ligase HOIP specifies linear ubiquitin chain assembly through its RING-IBR-RING domain and the unique LDD extension. *EMBO J.* 31 (19), 3833–3844. doi:10.1038/emboj.2012.217

Stieglitz, B. (2022). HHARI in motion reveals an unexpected substrate recognition site for RBR ligases', *Structure. Elsevier Ltd.* 30 (9), 1221–1223. doi:10.1016/j.str.2022.08.002

Stieglitz, B., Morris-Davies, A. C., Koliopoulos, M. G., Christodoulou, E., and Rittinger, K. (2012). LUBAC synthesizes linear ubiquitin chains via a thioester intermediate', *EMBO Reports. Nat. Publ. Group* 13 (9), 840–846. doi:10.1038/embor.2012.105

Stieglitz, B., Rana, R. R., Koliopoulos, M. G., Morris-Davies, A. C., Schaeffer, V., Christodoulou, E., et al. (2013). Structural basis for ligase-specific conjugation of linear ubiquitin chains by HOIP', *Nature. Nat. Publ. Group* 503 (7476), 422–426. doi:10.1038/nature12638

Tokunaga, F., Nakagawa, T., Nakahara, M., Saeki, Y., Taniguchi, M., Sakata, S. i., et al. (2011). SHARPIN is a component of the NF-κB-activating linear ubiquitin chain assembly complex', *Nature. Nat. Publ. Group* 471 (7340), 633–636. doi:10.1038/nature09815

Walden, H., and Rittinger, K. (2018). RBR ligase-mediated ubiquitin transfer: A tale with many twists and turns. *Nat. Struct. Mol. Biol.* 25 (6), 440–445. doi:10.1038/s41594-018-0063-3